Polymer Chemistry

Accepted Manuscript

ROYAL SOCIETY OF CHEMISTRY

www.rsc.org/polymers

Journal Name

ARTICLE

Durable Anion conducting Membrane with Packed Anion-exchange Sites and Aromatic Backbone for Solid-state Alkaline Fuel Cells

froReceived 00th January 20xx,
Accepted 00th January 20xx

DOI: 10.1039/x0xx00000x

www.rsc.org/

G. S.Sailaja[a,b],Shoji Miyanishi[a,b]and Takeo Yamaguchi[a,b] *

Abstract: Contemporary design strategies aimed at developing high functional anion conducting membranes (**ACM)s** for solid state alkaline fuel cell (**SAFC**) applications are often hampered by intrinsic limitations such as less efficient in controlling swelling, declined alkaline durability, high fuel cross-over and/or poor stability against OH radicals especially for polyelectrolytes composed of aliphatic chains. Hence, it is a challenging task to develop an **ACM** that satisfies all pre-requisites: high conductivity, alkaline durability, chemical stability and exhibiting very low fuel cross-over for successful **SAFC** applications. Here we present the systematic design of a simple molecular architecture based on benzyl ammonium group and benzene without hetero atom segment as a promising alkaline durable **ACM** with high anion conductivity. We have designed a new monomer 1,3,5-tri[*p*-(*N′,N″*-dimethylaminomethyl) phenyl]benzene (**TDAMPB**) with three tertiary amino groups that generates poly-**TDAMPB** (**PTDAMPB**) with three anion-exchange sites per molecule upon *in situ* cross-linking. This highly cross-linked aromatic polyelectrolyte could generate highly packed anion-exchange sites by polymerization in the pores of a porous substrate and thereby presents an imperative solution for the existing challenges associated with current **SAFC** membranes. The **PTDAMPB** membrane performances were compared with an aliphatic poly(vinylbenzyltrimethyl ammonium chloride) (**PVBTAC**) membrane. Results demonstrate that **PTDAMPB** membrane exhibited high OH^- ion conductivity similar to **PVBTAC** membranes, but exceptionally low methanol permeability and low swelling while maintaining good durability against hot alkali, boiling water and oxidative decomposition in contrast with **PVBTAC**. The functionalities of **PTDAMPB** membrane satisfy the anticipated requirements for a viable **SAFC**, which is difficult to attain simultaneously for a conventional anion-conducting membrane and hence results of this work address a major unresolved challenge representing an advancement toward successful **SAFC** applications.

Introduction

Fuel cells are a promising, green alternative option to the prevailing challenge of the world's increasing energy demands.[1] Proton-exchange fuel cells (**PEFCs**) possess intrinsic advantages of lower operating temperatures, compact sizes, portability, high-efficiency and zero emissions;[2] nevertheless, the operating window of **PEFCs** is narrow because of their inherent expensive nature that stems primarily from the requirement of Pt-based catalysts[3] and hydrogen cylinders/stations.[4] Solid-state alkaline fuel cells (**SAFCs**) are welcomed in this context with greater significance and enthusiasm because they offer several advantages and improved efficiency over **PEFCs** as a result of their remarkable cell reaction kinetics,[5] freedom to employ most of the non-noble-metal-based catalysts[6,7] and feasibility of using liquid fuels such as alcohol and ammonia, resulting in greater energy density and improved convenience.[8,9]However, the better success of **SAFCs** can be accomplished only through the use of a high performance anion-conducting membrane (**ACM**) that simultaneously exhibits a high ionic conductivity and high durability in hot alkaline environments and radical attack based on H_2O_2 formation through electrochemical reactions. In addition, limited fuel cross-over is also needed; the development of **ACMs** that satisfy all of these requirements represents a challenging task.

Higher ion exchange capacity of the membrane is generally beneficial for higher ion conductivity. One of our recent studies demonstrated that packed ion exchange site is suitable for high ion conduction with low content of water and has a distinctive proton conduction mechanism due to acid–acid interactions.[10]Hence a molecular design consisting of packed anion exchange sites could be a better choice for enhanced anion conduction for **SAFC** application. However, design strategies aimed at developing **ACMs**

[a]Chemical Resources Laboratory, Tokyo Institute of Technology, Nagatsuta 4259, Midori-ku, Yokohama, Kanagawa 226-8503, Japan
[b]Core Research for Evolutionary Science and Technology, Japan Science and Technology Agency, (JST-CREST)

with higher ion-exchange capacity (**IEC**) by incorporating multiple ionic sites as labile groups[11] or anchored to the polyelectrolyte backbone[12]indigenously trigger increased water uptake/swelling, causing prominent loss of mechanical properties and ultimately declined durability of the membrane.[13-16]

Durability is another important factor in the SAFC applications. Firstly, systematic material design is crucial for practical application. Aliphatic **ACMs** with high cross-linking and high **IEC** such as Poly(vinylbenzyltrimethyl ammonium chloride) (**PVBTAC**) can be fabricated by simple technology. However, such materials often suffered from poor durability against OH radical which is produced under fuel cell operating conditions.[17,18]**ACMs** with aromatic backbone have radical durability; however, most of the materials suffered from poor alkaline stability. Recent study showed that benzyl trimethyl ammonium group itself has relatively high stability against alkaline solution but poor stability if this group was attached to poly-sulfone or other polyarylene-ethers.[19,20]From this result, it is expected that simple structure based on benzyl ammonium group and benzene without hetero atom segment would be a promising alkaline durable membrane.

Finally, fuel cross-over through the membrane should be minimized to improve efficiency of **SAFC**. Swollen membrane enhance fuel cross-over, which leads to severe voltage reduction and catalyst poisoning[21] and is a major obstacle in the effective utilization of high-energy-density fuels in **SAFCs** and also a major limitation to the prospects of direct methanol fuel cells (**DMFCs**).[22] Suppression of the membrane swelling is also important to reduce the cross-over. Cross-linking of the membrane is an effective strategy for suppressing swelling. However, contemporary cross-linked membranes often hampered by limitations because either the cross-links are established at the expense of anion exchange groups or are less efficient in controlling swelling. [23-27]Our group has reported several pore-filling ion exchange membranes[28-31]where an inert and thermally stable porous substrate is used to fill the polyelectrolyte in the pores. The pore-filling structure is effective to suppress the membrane swelling

In this work, we have designed a new aromatic anionic electrolyte precursor, 1,3,5-tri[*p*-(*N′*,*N″*dimethylaminomethyl)phenyl] benzene (**TDAMPB**). This monomer has three tertiary amino groups, which can be converted to three benzyl trimethylammonium anion-exchange groups upon *in situ* cross-linking with *α,α′*-dichloro-*p*-xylene to forming the highly cross-linked and high **IEC** polyelectrolyte (**PTDAMPB**).**PVBTAC** a simple, highly conducting anionic electrolyte[32-34] conventionally fabricated by grafting or similar procedures was used as the reference membrane for comparison with **PTDAMPB** membranes. Both monomers were polymerized inside pores of porous substrate to suppress the membrane swelling. Figure 1 presents a schematic illustration of the **ACM** constituted with **PTDAMPB** polyelectrolyte having highly cross-linked rigid structure with packed anion exchange sites that preferentially enable transport of OH^- ions while simultaneously act as a barrier for methanol cross-over.

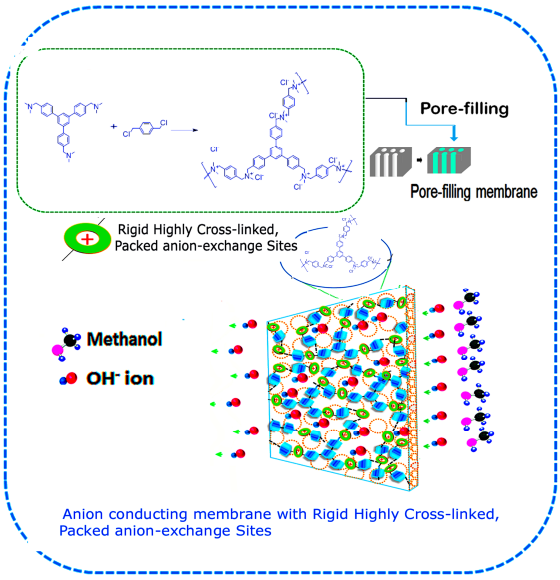

Figure1 Schematic illustration of **PTDAMPB** polyelectrolyte membrane with highly cross-linked rigid aromatic packed anion-exchange sites that enable high OH^--ion transport, simultaneously restricting methanol cross-over.

Experimental

E1. Materials: All reagents for the synthesis were used as received from the provider. The polyethylene porous substrate was provided by Toray Battery Separator Film Co Ltd., Japan (**V25EKD**; thickness 25 ± 1 µm, porosity = 46%, maximum pore size = 150 nm).

E2. Synthesis of 1,3,5-tri[p-(N′,N″ dimethylaminomethyl)phenyl] benzene

1,3,5-Tri(*p*-bromophenyl)benzene (**1**)

A mixture of 4-bromoacetophenone (19.9g, 100 mmol) and TsOH-H_2O (1.72g, 10mmol) was placed in a 2-necked 100mL round-bottom flask and stirred at 135°C for 24 h under nitrogen atmosphere. When the reaction was completed, 1.5L of dichloromethane (DCM) was added to the mixture, followed by neutralization with 1 M NaOH aq. The organic layer was extracted and subsequently washed with water (300mL × 3). The DCM in the organic layer was evaporated under vacuum. The residue was dispersed in hot toluene (80°C, 50mL), and the solid crystals were collected by filtration. This process was repeated twice, and the obtained solid was dried under vacuum to yield 1,3,5-tri(*p*-bromophenyl)benzene (11.59g, 21.3mmol) as yellowish, needle-like crystals in 64% yield.

^{1}H-NMR (400 MHz, $CDCl_3$): δ 7.69 (s, 3H), 7.61 (d, 6H), 7.53 (d, 6H)

1,3,5-Tri(*p*-cyanophenyl)benzene (**2**)

A mixture of 1,3,5-tri(*p*-bromophenyl)benzene (5.43 g, 10 mmol) and CuCN (3.49 g, 39.0 mmol) was refluxed in anhydrous dimethyl formamide (DMF) (50mL) for 36 h under a nitrogen atmosphere. The reaction mixture was then cooled and treated with distilled water (100mL) and ethylenediamine (15mL). The solid material was collected by filtration and dissolved in DCM (2.0L). The organic layer was washed with 10% ammonia aq. solution several times until the blue colour in the aqueous layer completely disappeared. The organic layer was washed with distilled water three times (200mL × 3), and the solvent was allowed to evaporate under reduced pressure. The residue obtained was dried under vacuum to yield 1,3,5-tri(*p*-cyanophenyl)benzene(3.47 g, 9.1mmol) as a white solid in 91% yield.

^{1}H-NMR (400 MHz, $CDCl_3$): δ 7.82-7.76 (m, 12H)

1,3,5-Tri(*p*-aminomethylphenyl)benzene (**3**)

1,3,5-Tri(*p*-cyanophenyl)benzene(3.0g, 7.87 mmol) was dispersed in anhydrous THF (50mL), and 2.5 M $LiAlH_4$ solution in anhydrous tetrahydrofuran (THF) (18.9mL) was added drop wise under nitrogen atmosphere. The reaction mixture was heated at 50°C for 24h. The reaction was initially quenched with water (2mL), and 15% NaOHaq. (2mL) and water (2mL) were subsequently added. The mixture was filtered and washed with THF (100mL). The solvent in the filtered solution was evaporated, and the obtained residue was dissolved in DCM and then washed with water. The solvent in the organic layer was evaporated, and the residue was dried under vacuum to yield 1,3,5-tri(*p*-aminomethylphenyl)benzene (2.63g, 6.68mmol) as a light-yellow, sticky solid in 85% yield.

^{1}H-NMR (400 MHz, $CDCl_3$): δ 7.76 (s, 3H), 7.67 (d, 6H), 7.42 (d, 6H), 3.95 (s, 6H)

1,3,5-Tri[*p*-(*N,N'*-dimethylaminomethyl)phenyl]benzene (**TDAMPB**)

A mixture of 1,3,5-tri(*p*-aminomethylphenyl)benzene (2.60g, 6.61mmol), formic acid (9.12g), and 37% formaldehyde aqueous solution (16.1g) was refluxed for 12 h. After cooling, the reaction mixture was concentrated under vacuum, and the residue was extracted with DCM. The organic layer was treated with 1 M NaOH aq. and subsequently washed with distilled water three times. The DCM was evaporated, and the residue obtained was dried under vacuum to yield 1,3,5-tri[*p*-(*N′,N″*-dimethylaminomethyl)phenyl] benzene (2.87g, 6.02mmol) as a light-yellow, sticky solid in 91% yield.

^{1}H NMR (400 MHz, $CDCl_3$): δ 7.77 (s, 3H), 7.65 (d, 6H), 7.41 (d, 6H), 3.49 (s, 6H), 2.29 (s, 18H)

*E3. Fabrication of anion-conducting membrane from **TDAMPB**:*

PTDAMPB membrane was fabricated by polymerization and *in situ* cross-linking in the pores of a polyethylene porous substrate. **TDAMPB** monomer solution in THF (0.1 mg/ml) was filled in the pores of V25EKD (thickness 25 ± 1 μm, porosity = 46%, maximum pore size = 150 nm) and the solvent was allowed to evaporate. Cross-linking reaction was performed by dropping *α,α'*-dichloro-*p*-xylene (cross-linker) solution in THF (Monomer-to-cross-linker molar ratio is 1.0:3.0) at room temperature for 3h, followed by a post-curing for 48h at 60°C to complete the reaction. The membranes were washed with Reverse Osmosis (RO) water followed by THF to remove any unreacted monomer and/or excess polymer. The membranes (Cl^-form) were converted into OH^-form by immersion in 1 M KOHaq. followed by washing with RO water for several hours inside a glove box to avoid CO_2 poisoning; the hydroxide-anion conductivity was subsequently measured.

The filling ratio Φ_f(%) of the polyelectrolyte was calculated using the following equation:

$$\Phi_f = \frac{W_{mem} - W_{sub}}{W_{sub}} \times 100$$

Where W_{mem} and W_{sub} are the dry-weight of the membrane and substrate (g), respectively.

*E4. Fabrication of **PVBTAC** membrane:* **PVBTAC** membranes were fabricated using the same polyolefin porous substrate by 'impregnation polymerization' technique using **VBTAC** and divinylbenzene as a cross-linker at 60°C for 16h, washed with RO water, dried at 60°C.

*E5. Ion-exchange capacity (**IEC**) measurements*: The **IEC** (meq/g) of the **ACM**s were measured using a potentiometric autotitrator (COM-1700, Hiranuma Sangyo, Japan). The Cl^-forms of the **ACMs** were exchanged to OH^-forms by immersion in a 1M KOH solution for 3h under stirring. After the membrane was removed from the solution, the pH of the solution was adjusted to around 2.0by adding HNO_3aq and the solution was titrated against 0.01 M $AgNO_3$aq. The IEC was calculated by the following equation.

$$IEC = \frac{mmol\ of\ quaternary\ ammonium\ groups}{Molecular\ weight\ of\ unit\ polymer}$$

E6. Ionic conductivity measurements: The in-plane Cl^- ion conductivities of the **ACMs** were measured using two-probe alternating-current electrochemical impedance spectroscopy (Solartron 1260, TOYO Corporation, Japan) at temperature from 30 to 80°C at 100% R.H. in the frequency range from 0.01 to 10^6 Hz. The membrane was clamped between a two-probe cell consisting of humidity chamber (SH-241, ESPEC, Japan) to attain the prescribed temperature and humidity conditions, and measurements were performed.

The ion conductivity of the membrane was calculated according to the equation

$$\sigma = \frac{d}{R_{bulk} \cdot l \cdot w}$$

Where σ is the ion conductivity (S/cm), $R_{bulk}$is the membrane resistance (Ω), *d* is the length between two Pt plates (cm), *l* and *w* are the thickness and width of the membrane (cm), respectively.

OH^- ion conductivity measurement: The membranes (Cl^-form) were converted into OH^-form by immersion in 1 M KOHaq. followed by washing in RO water for several hours inside a glove box to avoid CO_2 poisoning. The hydroxide-anion conductivity was subsequently measured using two-probe alternating-current electrochemical impedance spectroscopy under Nitrogen atmosphere in a specially designed humidity chamber consisting of two-probe cell to attain the prescribed temperature and humidity conditions to avoid CO_2 poisoning. The conductivity was measured at temperature from 30 to 70°C at 100% R.H. in the frequency range from 0.01 to 10^6 Hz using the above equation.

E7. Water-content measurements: The water uptake of the membrane was measured usinga MSB-ADV-FC system (BEL Japan, Inc.). The samples were pre-treated under vacuum at 60°C for 1 h.

E8. Methanol permeability measurement: The permeability of the **PTDAMPB** and **PVBTAC** membranes were measured at 25°C with a special H-type diffusion cell composed of two chambers. Chamber I was filled with pure water, and chamber II was filled with 10 wt.% methanol aq.; both the water and methanol solution were continuously stirred and the methanol/water solution was separated by the membrane. The amount of permeated methanol on the water side and the corresponding feed concentration of methanol (as a control) were measured at regular time intervals using gas chromatography. The time lag (ϑ) and permeability constant [$cm^2 \cdot s^{-1}$] were determined by the slope of plot of the change in the permeated methanol concentration as a function of time.

E9. Fenton's test: Small pieces of dried membrane samples of **PTDAMPB** and **PVBTAC** (Cl^- form) were soaked in Fenton's reagent (3wt.% H_2O_2 aqueous solution containing 3 ppm $FeSO_4$) in air-tight brown bottles at 60°C under stirring. After certain intervals of time, the membranes were removed; any excess water on the surface was wiped off using wet filter paper, and the membranes were dried under vacuum at 60°C for 4h. The sample weights were immediately recorded using a microbalance. This procedure was repeated three times to ensure reproducibility.

E10. Confocal Raman measurement:

Confocal Raman line mapping of the membrane was measured by NRS-5100 (Nihon bunko. Corp.)with 532 nm excited wavelength and 50 μ m slit width. The spectrum along depth of the membrane with 1μ m interval was integrated twice by using 5-10mW intensity laser.

E11.Mechanical Property Evaluation:

Tensile stress versus strain evaluations of membranes were performed at 23 °C using 55R-5867 (Instron corp.) test machine operating at a strain rate of 100 mm/min. Three samples with 50 mm distance between chucks were tested to ensure of good reproducibility of the results.

Results and discussion

Scheme 1 shows synthetic method of **TDAMPB** polyelectrolyte precursor.

Scheme 1[a]

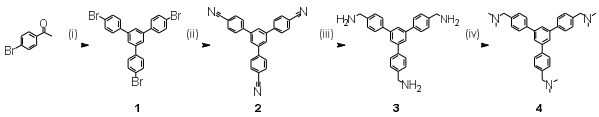

[a]Reagent and conditions:(i) TsOH-H_2O, 135°C; (ii) CuCN, DMF, reflux; (iii) LAH, THF, 50°C; (iv) HCOOH,HCOH, reflux

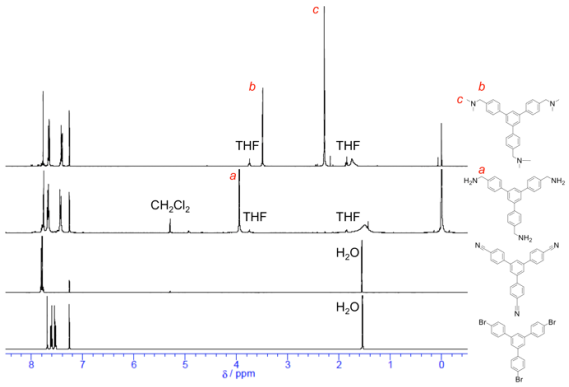

Figure 2[1]H-NMR spectra of **1**,**2**,**3** and **TDAMPB** in $CDCl_3$

Briefly, 1,3,5-tribromophenyl benzene (**1**) was synthesized from 4-bromoacetophenone by acid-catalyzed condensation[35]. The bromide group of **1** was converted to nitrile group by using CuCN[36] and then reduced to primary amine group by using $LiAlH_4$ solution to obtain **3**. Finally, primary amine group was selectively converted to tertiary amine group by Eschweiler-Clarke reaction to form **TDAMPB**.

The ^{1}H NMR spectra of **TDAMPB** and its synthetic intermediates are shown in Figure 2.This spectra confirm the successful synthesis of each product and purity of **TDAMPB**. It is to be noted that **TDAMPB** can be obtained at acceptable yield (total 45%) from commercially available 4-bromoacetophenone and scaling up of this material is easy.

Next, the **PTDAMPB** membrane was fabricated by polymerizing **TDAMPB** and in-situ cross-linking with *α,α'*-dichloro-*p*-xylene. **PVBTAC** membrane was also fabricated in similar manner by polymerizing **VBTAC** with 1wt.% divinyl benzene as cross-linker and both membranes were characterized. Assuming the polymer density as 1 g.cm^{-1} and taking into porosity of the substrate (46vol.%), almost all of the pores were filled with polyelectrolyte in both membranes. The polymerization scheme of **TDAMPB** and **VBTAC** are shown as scheme 2 and 3 respectively.

Scheme 2 Polymerization of **TDAMPB** and *α,α'*-dichloro-*p*-xylene

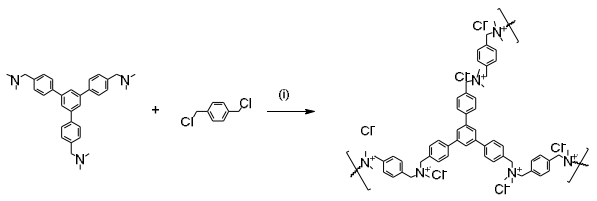

[a]Reagent and conditions:(i) 60 °C, THF

Scheme 3 Polymerization of **VBTAC** in presence of divinylbenzene

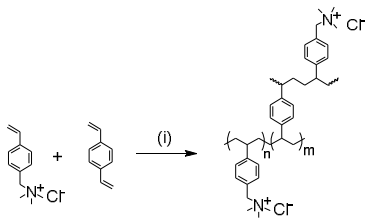

[a]Reagent and conditions:(i) 60 °C, ***V50***

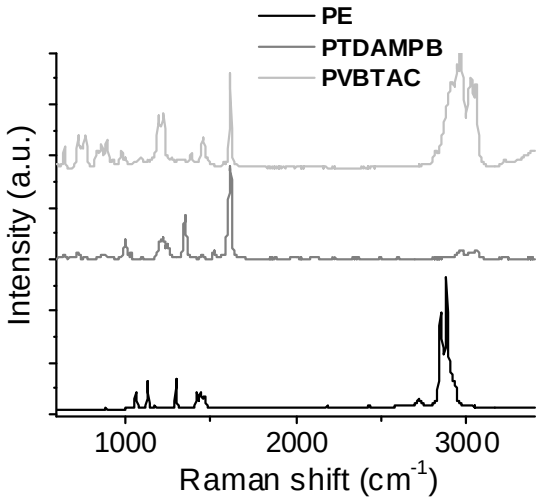

Figure 3(A) Confocal-Raman spectra of polyethylene porous substrate, **PVBTAC** bulk polymer and **PTDAMPB** bulk polymer

The Confocal-Raman spectra of polyethylene porous substrate, **PVBTAC** bulk polymer and **PTDAMPB** bulk polymer are provided as Figure 3A. The confocal-Raman spectra along the cross-section of the **PTDAMPB** (Figure 3B) and **PVBTAC** (Figure 3C) membranes in the region of 1500 cm^{-1} to 1700 cm^{-1}also confirm the filling of polyelectrolytes. The Raman shift at 1610 cm^{-1}derived from the aromatic domains of **PVBTAC** or **PTDAMPB** confirms the presence

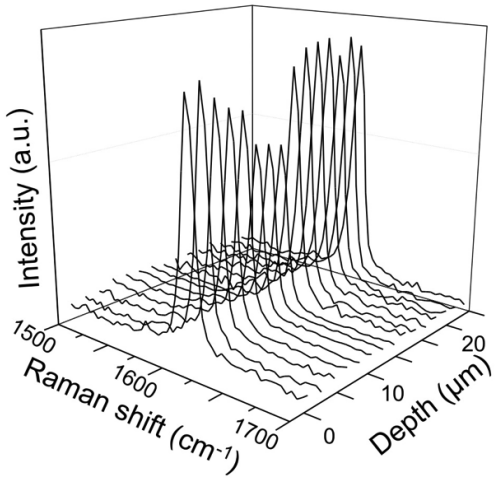

(B)

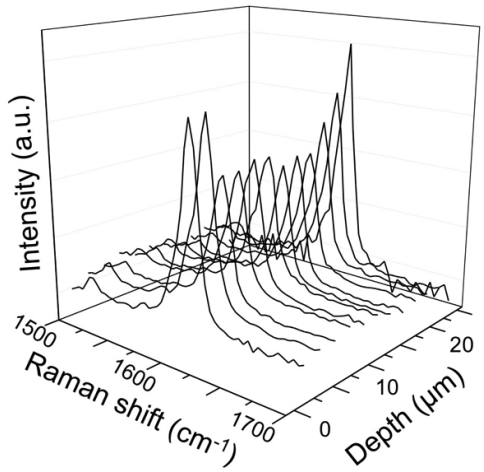

(C)

Figure 3(B) Confocal-Raman spectra depth profile of **PTDAMPB** and **(C) PVBTAC** membranes normalized to the peak at 2873 cm^{-1}

of the polyelectrolyte, whereas the uniformity of the relative intensity in the depth profile is correlated to uniform filling of the polyelectrolyte in the pores of the porous substrate. The Raman shift at 2873cm^{-1}corresponds to alkyl domains in polyethylene. The complete spectra of the membranes are provided in Figure S1.

The conversion of reaction site in **TDAMPB** monomer is critical because it determines the **IEC** and cross-link density of the material; at the same time it is also an important parameter for ionic conductivity, durability and permeability of **ACM**. The **IEC** of the **PTDAMPB** and **PVBTAC** membranes were determined as 1.98 and 2.26 meq.g^{-1} respectively by titration. Since half of the membrane weight is dominated by polyethylene substrate, **IEC** of the filled polyelectrolyte itself is 3.96 and 4.52meq.g^{-1}, respectively which is in good agreement with the theoretical values of **PTDAMPB** and **PVBTAC** solid polyelectrolytes (4.06 and 4.74 meq.g^{-1}, respectively). This result indicates almost complete quantitative conversion of the reaction sites in **TDAMPB** monomer. The same conclusion was also obtained by elemental analysis of the membrane.

Figure 4 presents the water uptake comparison of **PVBTAC** and **PTDAMPB** membranes. Although most of the conventional **ACMs** with high **IEC** and high conductivity are suffered from problems due to significant swelling, the **PTDAMPB** membrane exhibited only lower water uptake (19.9 wt.% at 90% R.H.) in contrast to **PVBTAC** membrane which is extremely lower when compared to a typical anion exchange membrane with similar ion exchange capacity (Figure 4, Table 1). **Table 3** shows the physical property variation data of PTDAMPB and PVBTAC membranes as a function of area and thickness change under swollen state demonstrating that the change in dimensions for these membranes are not significant.

It is to be noted that despite of highly cross-linked structure, **PTDAMPB** membrane can exchange anion by simply soaking in corresponding salt solution. This is evidenced by comparing elemental analysis data (Table 2). The energy-dispersive X-ray analysis (EDX)-elemental mapping data of the membrane before and after ion exchange reaction further corroborate the conversion Cl^- ions to Br^- ions (Figure 5).

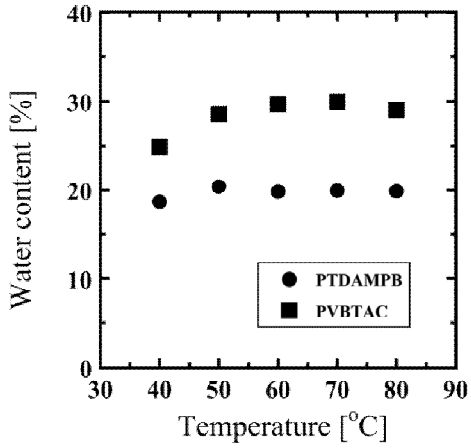

Figure 4 Water uptake of **PVBTAC** and **PTDAMPB** membranes.

Table 1 Physical property of **PTDAMPB** and **PVBTAC** membrane

Membrane	IEC[a] (meq/g)	Water[b] Uptake (wt%)	Ion conductivity[c] (mS/cm) Cl^-	OH^-	Methanol permeability (mol m/m^{2}s)
PTDAMPB membrane	1.98	20	64	86	1.0×10^{-7}
PVBTAC membrane	2.26	30	69	91	1.2×10^{-6}

[a]measured by titration, [b]at 80°C under 90% R.H. [c]70°C under 100% R.H.

Table 2 Elemental analysis data of **PTDAMPB** membranes

Component	Value	H (wt%)	C (wt%)	N (wt%)	Cl (wt%)	Br (wt%)
PTDAMPB membrane (Cl^-)	Theoretical	10.7	79.3	2.8	7.2	0.0
	Observed	9.6	73.1	2.6	8.6	0.0
PTDAMPB membrane (Br^-)	Theoretical	10.1	73.7	2.4	0.0	13.7
	Observed	10.1	70.5	2.1	0.0	12.4

[a]The value was calculated assuming that filled **PTDAMPB**: polyethylene substrate = 1.0:1.0 wt. ratio

Table 3 Physical property variation data of membranes under swollen state

Membrane	Physical property variation under swollen condition	
	Change in area (%) Average	Change in thickness (%) Average
PTDAMPB	0.0332	0.1569
PVBTAC	0.0558	0.2546

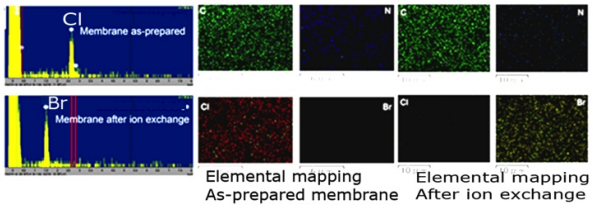

Figure 5 FESEM-EDX elemental mapping of as-prepared (Cl^- form) and substituted (Br^- form) of **PTDMAPB** membrane. The EDX spectrum and elemental mapping of the as-prepared membrane shows strong peaks corresponding to Cl^- in the membrane. After ion exchange with Br^-, strong peaks of Br^- were detected, with the absence of any Cl^- peaks, confirming that all the Cl^-ions were substituted with Br^- ions.

The stress-strain curves of PTDAMPB and VBTAC membranes are shown in figure 6A and 6B respectively. It is well known that good mechanical properties are essential for ACMs to be successful for fuel cell applications. The results indicate excellent tensile strength values for both **PTDAMPB** (1370 kgf/cm^2) and **PVBTAC** (1048 kgf/cm^2) membranes compared with typical **ACM**s.

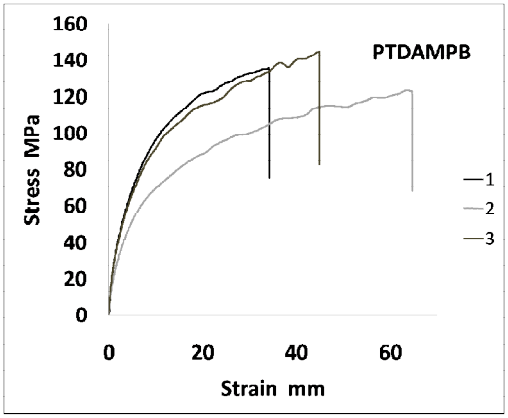

Figure 6(A) The stress-strain curves of **PTDAMPB** membranes

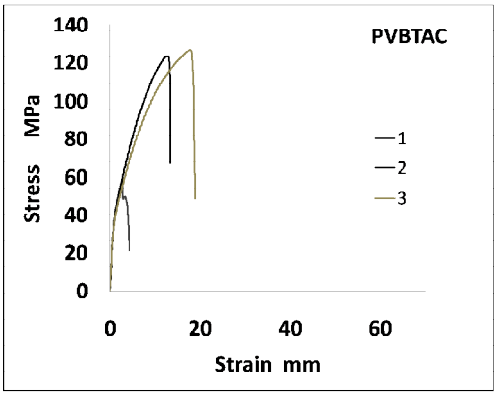

Figure 6(B) The stress-strain curves of **PVBTAC** membranes

It is to be noted that in contrast to **PVBTAC**, **PTDAMPB** has highly cross-linked structure without losing ion exchange capacity reflecting its molecular design. The high **IEC** value of the membrane is beneficial for high ionic conductivity, as demonstrated in Figure 7A. The ionic conductivity chart implies a linear relationship between the conductivities and temperature with activation energy of 29.1 and 19.3 kJ/mol for Cl^- and OH^- ions respectively. High ion conductivity values of 64 and 86 mS/cm (at 70 °C) was obtained in the $Cl^-$and OH^- form of **PTDAMPB** membrane.

Chemical durability of the membrane is important issue for the practical application. Figures 7B and 7C confirm that **PTDAMPB** membrane shows little conductivity change after soaking in boilingwater for 72h and in 1 M KOH aq. at 60 °C for 30 days, indicating high thermal and alkaline durability of the material.

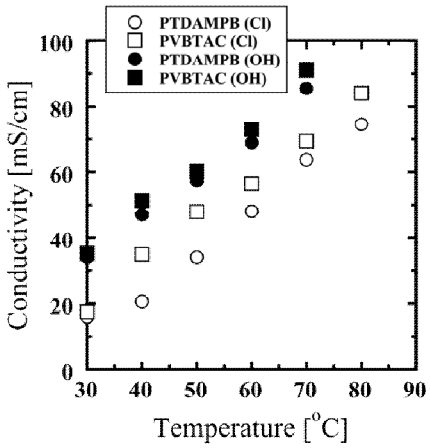

Figure 7(A) Cl^- and OH^-ion conductivity of **PTDAMPB** and **PVBTAC** membranes at 100% R.H. as a function of temperature

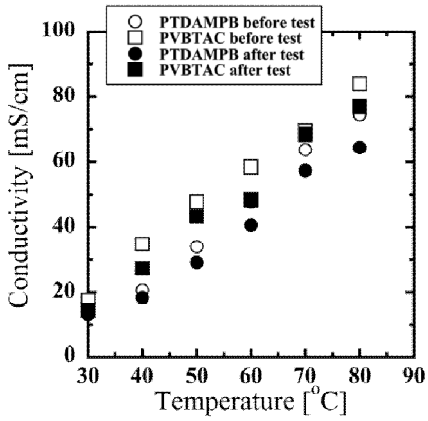

Figure 7(B) Cl^--ion conductivity of **PTDAMPB** and **PVBTAC** membranes at 100% RH after durability test in boiling water for 72 h

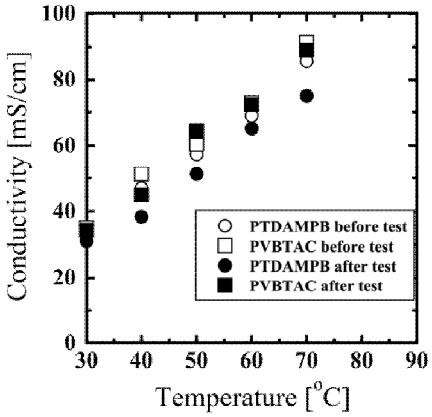

Figure 7(C) OH^--ion conductivity profile of PTDAMPB and PVBTAC membranes at 100% RH after durability test in 1 M KOH aq. at 60 °C for 30 days.

Figure 8 provides information related to the responses of oxidative decomposition against OH radicals by Fenton's reaction. A weight change was hardly observed for the **PTDAMPB** membrane at 60 °C even after 8h, whereas **PVBTAC** lost 74 wt.% by that time. In addition to the basic rigid aromatic configuration, the highly cross-linked structure of **PTDAMPB**, analogous to typical thermosetting polymer also significantly contributes to the better oxidative stability of **PTDAMPB ACM**.

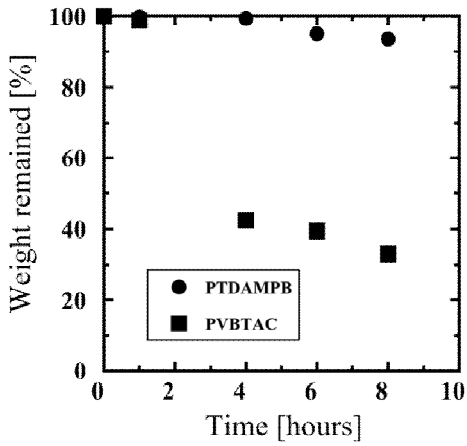

Figure 8 Weight change of **PTDAMPB** and **PVBTAC** membranes as a function of reaction time in Fenton's durability test

Although both membranes exhibit similar ionic conductivities, the results corroborate superior chemical stability and durability of **PTDAMPB** compared to **PVBTAC**. The **PTDAMPB** polyelectrolyte is structurally analogous to thermosetting engineering plastics like melamine formaldehyde, which has high strength and poor water absorption. Hence, the water uptake of the **PTDAMPB** membrane is greatly diminished irrespective of its higher **IEC**, reflecting its molecular structure.

Methanol permeability is a key concern in liquid fuel **SAFCs** because methanol cross-over adversely affects cell performance. When methanol cross-over occurs, the methanol reacts with the cathode catalyst. Eventually, catalyst poisoning leads to severe voltage reduction and mixed potential loss at the cathode. Hence, when Nafion is used in a **DMFC**, typically only less than 10 wt.% methanol solution can be used as fuel to reduce the methanol cross-over effect and thereby achieve high cell performance.[37]

An **ACM** with significantly lower methanol permeation has key advantages because of the amplified efficiency achieved with such membranes.[38]The methanol permeability of **PTDAMPB** and **PVBTAC** membrane was experimentally measured and analysed by knowing the diffusion coefficient and time lag for diffusion..

The time lag (θ) for diffusion and the mutual diffusion coefficient (D) for the **ACMs** are related through equation (i):

$$D = \frac{L^2}{6\theta}$$

.....Equation (i)

Where 'L' represents the thickness of the membrane and 'θ' the time lag.[31]

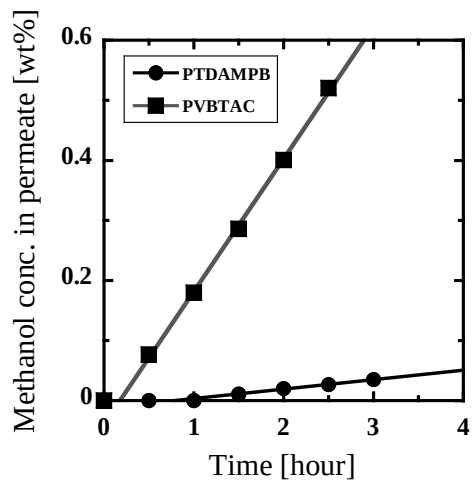

Figure 9(A) Time dependence of methanol concentration in permeate through **PTDAMPB** and **PVBTAC** membranes as a function of time.

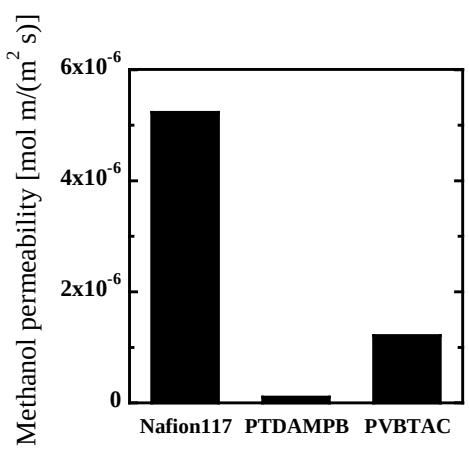

Figure 9(B) Comparison of the methanol permeability of **PTDAMPB**, **PVBTAC** and **Nafion117** membranes at 25 ^{0}C.

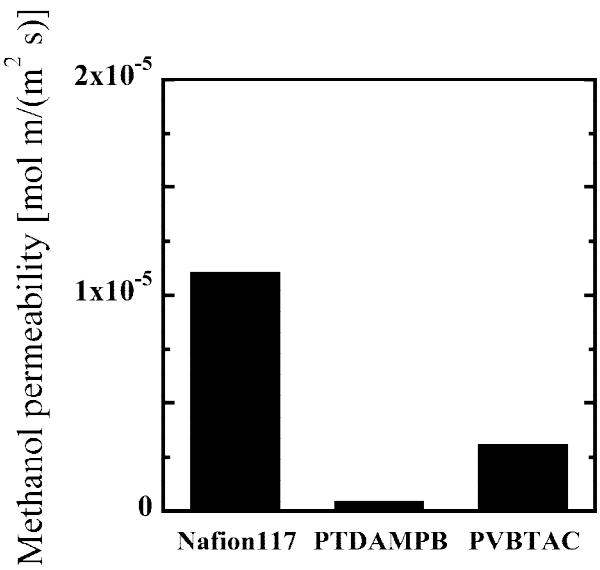

Figure 9(C) Comparison of the methanol permeability of **PTDAMPB**, **PVBTAC** and **Nafion117** membranes at 60 ^{0}C.

Figure 9A shows methanol concentration change in permeate through the membranes as a function of time. **PTDAMPB** membrane shows significantly lower concentration change compared with **PVBTAC** membrane. It is also noted that a significant time lag for diffusion was observed in **PTDAMPB** membrane indicating a lower diffusion coefficient in the membrane. From this result, the time lag, diffusion coefficient and permeability values for the **PTDAMPB** membrane were estimated as 2,800 s, 4.6×10^{-10} $cm^2.s^{-1}$ and 1.0×10^{-7} mol m/m^2s respectively, whereas the **PVBTAC** membrane exhibited time lag of 640 s and a diffusion coefficient of 2.1×10^{-9} $cm^2.s^{-1}$ and a permeability of 1.2×10^{-6}mol m/m^2s at 25^{0}C The permeability of **PTDAMPB** membrane is 1/10 of that of the **PVBTAC** membrane and as low as 1/53 as that of **Nafion117** membrane (Figure 9B). The methanol permeability comparison chart of **PTDAMPB**, **PVBTAC** and **Nafion117** membranes at 60 ^{0}C presented as figure 9C further demonstrate the excellent resistance of PTDAMPB membrane when compared to **PVBTAC** and **Nafion117** at practical fuel cell operating conditions.

The diffusion constant *D* of **PTDAMPB** membrane is five-fold lower than **PVBTAC** membrane and much lower than **Nafion 117** which shows no apparent time lag for diffusion. Therefore, the main factor that determines the methanol permeation difference is the difference in *D*. The diffusion coefficient of the membrane reflects the physicochemical characteristics of the membrane, especially its structure and cross-linking density. In the present scenario, difference in *D* between **PTDAMPB** and **PVBTAC** emphasizes the vital role of the rigid aromatic molecular structure and highly cross-linked architecture of **PTDAMPB** since both **PTDAMPB** and **PVBTAC** membrane were prepared by the same method.

As shown in Table 1, **PTDAMPB** absorb significantly less content of water despite of high ion exchange capacity of the material. This behaviour is unusual for typical polyelectrolyte membrane and leads to the formation of packed anion exchange site in the membrane. This packed anion exchange site could be suitable for anion conduction as similar to proton exchange membrane and contribute to high ion conductivity despite of low diffusion of the solute in the membrane as confirmed by significantly low fuel permeability (Figure 9) both at 25 ^{0}C and 60 ^{0}C. Therefore, the design concept presented here can be explored for the development of membranes which meets several characters such as high ion conductivity, high durability, and low permeability at the same time.

Conclusions

In conclusion, we have designed a new aromatic anionic electrolyte monomer **TDAMPB** with aromatic backbone and three tertiary amino groups per molecule, that is converted to three quaternary ammonium anion-exchange groups upon *in situ* cross-linking with *α,α′*-dichloro-*p*-xylene forming highly cross-linked and highly packed anion exchange sites. The anion conductive polyelectrolyte membrane **PTDAMPB** fabricated with **TDAMPB** satisfies most of the anticipated requirements for a **SAFC** membrane primarily due to its unique packed anion-exchange sites and aromatic structure. The **PTDAMPB ACM** exhibited high anion conductivity, exceptionally low methanol cross-over, high alkaline and radical stability, which is a challenging task to achieve by conventional approaches. Typical aliphatic **ACMs** like **PVBTAC** exhibiting high **IEC** and high ionic conductivity are generally designed with conventional cross-links and often suffered from higher water uptake, increased fuel cross-over and greater susceptibility to radical attack and are hence relatively less durable. Such antagonistic factors are the real challenges associated with designing smart anion-conducting membranes, and **PTDAMPB ACM** presents a new solution to these prevailing issues.

Acknowledgements

We gratefully acknowledge the financial support of Core Research for Evolutional Science and Technology (CREST) of the Japan Science and Technology Agency (JST) to perform this work. We also acknowledge Dr.Yuhei Oshiba and Dr.Hidenori Kuroki, Tokyo Institute of Technology for their extremely valuable support.

Notes and references

† Electronic Supplementary Information (ESI) available: [details of any supplementary information available should be included here]. See DOI: 10.1039/b000000x/

References

1. (a) B. C. H. Steele and A. Heinzel, *Nature* 2001, **414**, 345; (b) A. Kirubakaran, S. Jain and R. K. Nema, *Renewable and Sustainable Energy Rev.* 2009,**13**, 2430.
2. (a) Y. Wang, K. S. Chen, J. Mishler, S. C. Cho and X. C. Adroher, *Appl. Energy* 2011**, 88**, 981 (b)J.H. Wee, *Renewable and Sustainable Energy Rev.* 2007**, *11***, 1720.
3. (a) B. P. Vinayan , R. Nagar, N. Rajalakshmi and S. Ramaprabhu, *Adv. Funct. Mater*. 2012, **22**, 3519; (b) B. Genorio, R. Subbaraman, D. Strmcnik, D. Tripkovic, V.R. Stamenkovic and N.M. Markovic*, Angew. Chem. Int. Ed.*2011**, 50**, 5468.
4. A. T. Raissi and D. Block, *IEEE Power & Energy*, 2004, **2(6),** 43.
5. (a) S. D. Poynton, J. P. Kizewski, R. C. T. Slade and J. R. Varcoe, *Solid State Ionics*, 2010, **181**, 219. (b) J.S. Park, S.H. Park, S.D. Yim, Y.G. Yoon, W.Y. Lee and C.S. Kim, *J. Power Sources*, 2008,**178**, 620.
6. J.R. Varcoe and R.C.T. Slade, *Fuel Cells*, 2005, **5**, 187.
7. G. Merle, M. Wessling and K. Nijmeijer, *J. Membr. Sci.*, 2011, **377**, 1.
8. K. Asazawa, K. Yamada, H. Tanaka, A. Oka, M. Taniguchi and T. Kobayashi, *Angew. Chem. Int. Ed.,*2007, **46**, 8024.
9. E. Agel, J. Bouet and J. F. Fauvarque, *J. Power Sources*, 2001, **101**, 267.
10. T. Ogawa, T. Aonuma, T. Tamaki, H. Ohashi, H. Ushiyama, K. Yamashita and T. Yamaguchi, *Chem. Sci.***,** 2014,**5**, 4878.
11. J. Pan, S.F. Lu, Y. Li, A.B. Huang, L. Zhuang and J.T. Lu, *Adv. Funct. Mater*. 2010, **20**, 312.
12. N.J. Robertson, H.A. Kostalik IV, T.J. Clark, P.F. Mutolo, H.D. Abruna and G.W. Coates, *J. Am. Chem. Soc.* 2010, **132**(3400.
13. T.J. Clark, N.J. Robertson, H.A. Kostalik IV, E.B. Lobkovsky, P.F. Mutolo and G.W. Coates, *J. Am. Chem. Soc.* 2009, **131**, 12888.
14. J. Ni, C.J. Zhao, G. Zhang, Y. Zhang, J. Wang, W.J. Ma, Z.G. Liu and H. Na, *Chem. Commun.,* 2011,**47**, 8943.
15. J. Pan, Y. Li, L. Zhuang and J.T. Lu, *Chem. Commun*. 2010,**46**, 8597.
16. M. Kumar, S. Singh and V. K. Shahi, *J. Phys. Chem. B*, 2010, **114**, 198.
17. Y. T. Luo, J. C. Guo, C. S. Wang, D. Chu, *Electrochem. Commun.*,2012, **16**, 65
18. H. Zhang and P. K. Shen, *Chem. Rev.*, 2012, **112 (5),** 2780.
19. (a) J. R. Varcoe, P. Atanassov, D. R. Dekel, A. M. Herring, M. A. Hickner, P. A. Kohl, A.R. Kucernak, W. E. Mustain, K. Nijmeijer, K. Scott, T. Xuk and Lin Zhuang, *Energy Environ. Sci.,* 2014, **7**, 3135 (b) O. I. Deavin, S. Murphy, A. L. Ong, S. D. Poynton, R. Zeng, H. Herman and J. R. Varcoe, Energy Environ. Sci., 2012, **5(9)**, 8584.
20. a) C. G. Arges and V. Ramani, *Proc. Natl. Acad. Sci. U. S. A.,* 2013, **110 (7)**, 2490 (b) C. G. Arges and V. Ramani, *J Electrochem Soc,* 2013,**160**, F1006.
21. A. Heinzel and W. M. Barragan*, J. Power Sources*, 1999,**84**,70
22. A.S. Arico, S. Srinivasan and V. Antonucci, *Fuel Cells,* 2001, **1** (**2**), 133.
23. J. L. Qiao, J. Fu, L. L. Liu, L. Xu, Y. Y. Liu and J. W. Sheng, *Int. J. Hydrogen Energy,* 2012, **37**, 4580.
24. T. C. Zhou, J. Zhang, J. L. Qiao, L. L. Liu, G. P. Jiang, J. Zhang and Y. Y. Liu, *J. Power Sources*, 2013, **227**, 291.
25. a) B. Gurau and E. S. Smotkin, *J. Power Sources* 2002, **112**, 339.
26. L. J. Hobson, Y. Nakano, H. Ozu and S. Hayase, *J. Power Sources,* 2002, **104**, 79.
27. A. Kuver, K. Potje-Kamloth, *Electrochem. Acta,* 1998, **43**, 2527.
28. H. Jung, K. Fujii, T. Tamaki, H. Ohashi, T. Ito and T. Yamaguchi, *J. Membrane Sci.,* 2011, **373 (1-2)**, 107.
29. H. Hara, H. Ohashi, T. Ito, T. Yamaguchi, *J Phys Chem B*, 2009, **113 (14)**, 4656.
30. T. Yamaguchi, Z. Hua, T. Nakazawa and N. Hara, *Adv. Mater.*, 2007, **19 (4)**, 592.
31. T. Yamaguchi, S. Nakao and S. Kimura, *Macromolecules*, 1991, **24**, 5522.
32. N. S. Kwak, J. S. Koo and T. S. Hwang, *Macromol. Res.,* 2012, **20**, 205.
33. M.S. Lee, T. Kim, S.H. Park, C.S. Kim and Y.W. Choi, *J. Mater. Chem.,* 2012, **22**, 13928
34. S. M. Kolhe and A. Kumar, Radiation Phys. and Chem. 2005,**74**, 384.
35. Y. N . Zhao, J. A Li, C. J. Li, K. Yin, D. Y.Ye and X. S. Jia, *Green Chem.* 2010, **12**, 1370.
36. M. Dinca, A. Dailly, C. Tsay and J. R. Long, *Inorg. Chem.,* 2008, **47**, 11.
37. X. Ren, P. Zelenay, S. Thomas, J. Davey and S. Gottesfeld, *J. Power Sources,* 2000, **86**, 111.
38. (a) M. Kamiya, M. Y.Fujita, Y. Takeoka, M. Rikukawa, *Electrochimica Acta*, 2010, **55**(4),1385. (b) C. H. Lee, H.B. Park, Y. S. Chung, Y. M. Lee and B.D. Freeman, *Macromolecules*, 2006, **39 (2)**,755.

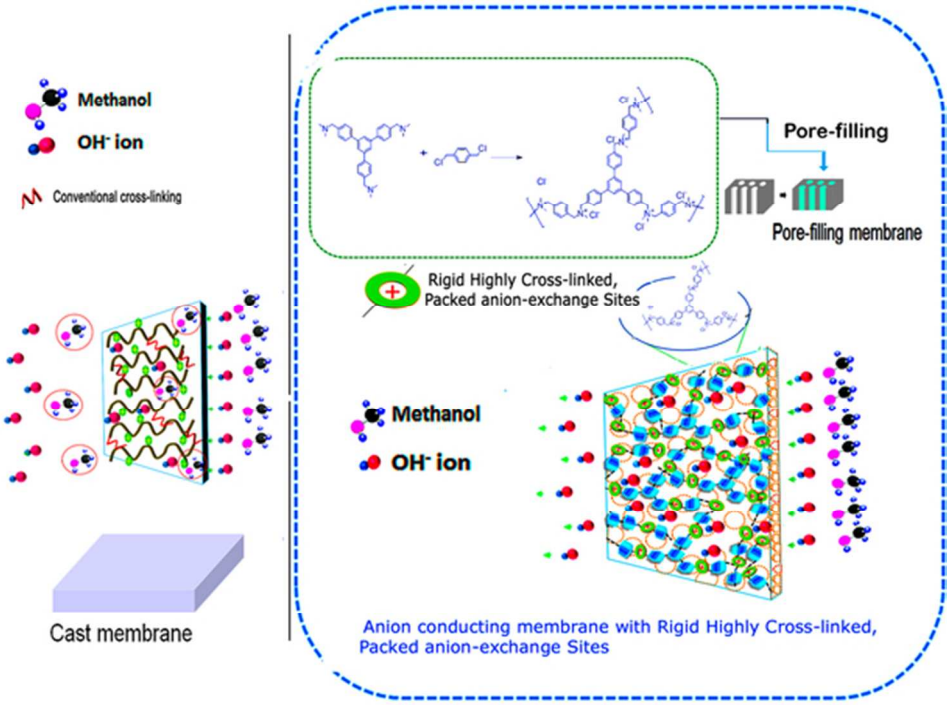

27x19mm (600 x 600 DPI)